

Tsunami Hazard and Inundation Modeling and Assessment for the U.S. Gulf Coast

A. Pampell-Manis* J. Horrillo† J. Figlus†

September 30, 2015

1 Introduction

Gulf of Mexico (GoM) coasts were included in the U.S. Tsunami Warning System in 2005. The warning system enables local emergency management to act in response to tsunami warnings. To plan for the warning response, emergency managers must understand what specific areas within their jurisdictions are threatened by tsunamis. Coastal hazard areas susceptible to tsunami inundation can be determined by historical events, by modeling potential tsunami events (worst-case scenarios), or by using a probabilistic approach to determine the period of recurrence or likelihood of exceeding a certain threshold. As the GoM coastal regions have no significant recent historical tsunamis records, numerical modeling and probabilistic methodologies for source identification must be used to determine these coastal hazard zones.

Potential tsunami sources for the GoM are local submarine landslides [ten Brink et al., 2009]; potential tsunami sources outside the GoM are considered a very low threat and may not significantly impact GoM coastal communities or infrastructure [Knight, 2006]. Although a massive underwater landslide in the GoM is considered a potential hazard, the probability of such an event is quite low [Dunbar and Weaver, 2008] and is related to ancient (historical) massive landslides which were probably active prior to 7,000 years ago when large quantities of sediments were emptied into the GoM. However, sediment continues to empty into the GoM mainly from the Mississippi River, contributing to slope steepening and the increase of fluid pore pressure in sediments, which may lead to slope instability and landslide activity. In addition, the unique geometry of the GoM basin makes even unlikely tsunami events potentially hazardous to the entire Gulf Coast. Waves tend to refract along continental slopes; thus, given the curved geomorphology of the GoM shelf and the concave shape of the coastline, any outgoing tsunami wave could potentially affect the opposite coast as well as the coast close to the landslide source.

Three large-scale ancient submarine landslides with tsunamigenic potential have been identified within the GoM [ten Brink et al., 2009], representing possible worst-case tsunami scenarios affecting GoM coasts in the past. In order to fill gaps along the continental shelf

*Department of Ocean Engineering, Dwight Look College of Engineering, Texas A&M University at Galveston, Galveston, TX, 77553, pampella@tamug.edu

†Department of Ocean Engineering, Dwight Look College of Engineering, Texas A&M University at Galveston, Galveston, TX, 77553

between these historical landslide sources and generate a more complete picture of landslide tsunami potential in the GoM, a probabilistic approach has been implemented to develop four additional synthetic landslide sources (full detail given in A. Pampell-Manis et al., *J. Geophys. Res. Oceans*, under review). Our probabilistic approach confirmed a recurrence period of major landslide events of around 8000 years, consistent with recent findings [Geist et al., 2013]. These probabilistic tsunami sources are used as the maximum credible events that could happen in a particular region of the GoM according to the local bathymetry, seafloor slope, and sediment information. The probabilistic maximum credible events together with the historical sources are then used as dynamic tsunami sources within coupled 3D and 2D numerical models to model tsunami generation and propagation throughout the GoM and to develop inundation maps within the inundation-prone areas of five selected communities along the Gulf Coast: South Padre Island, TX; Galveston, TX; Mobile, AL; Panama City, FL; and Tampa, FL.

Additionally, since vulnerability assessments are still essential for coastal locations where inundation studies have not yet been planned or modeled, or where little bathymetric and/or elevation data exist, we also aim to provide estimates of tsunami inundation zones in these locations. Inundation maps with even low resolution are useful to emergency managers to create first-order evacuation maps, and some methods currently exist to provide low-resolution estimates of hazard zones for regions which do not warrant high-resolution maps, e.g. the 10m (33ft) land elevation contour line. However, in low-lying coastal regions such as along the Gulf Coast, this elevation is too far inland to be applicable for estimating potential tsunami inundation zones. As a result, we are developing a methodology to compare tsunami inundation to hurricane storm surge data in order to provide a reference to hurricane hazard zones which are well-known to GoM emergency management. Even though many aspects of storm surge inundation are completely different from tsunami (time scale, triggering mechanism, inundation process, etc.), good correlations between tsunami inundation and storm surge flooding on a regional scale can be extrapolated to provide first-order estimates of potential tsunami inundation hazard in communities where detailed inundation maps have not yet been developed or are not possible due to unavailability of high-resolution bathymetry/elevation data.

Although the probability of a large-scale tsunami event in the GoM is low, our study has confirmed that submarine landslide events with similar characteristics to the ones modeled here have the potential to cause severe flooding and damage to GoM coastal communities similar to or even greater than that seen from major hurricanes, particularly in barrier island regions. This work is intended to provide guidance to local emergency managers to help with managing urban growth, evacuation planning, and public education with the vision to mitigate potential GoM tsunami hazards.

2 Inundation Modeling

2.1 Numerical Models

Tsunami wave development and subsequent propagation and inundation of coastal communities is modeled using coupled 3D and 2D numerical models. Tsunami generation by each submarine landslide is modeled using the 3D model TSUNAMI3D [Horrillo, 2006, Horrillo et al., 2013], which solves the finite difference approximation of the full Navier-Stokes equations and the incompressibility (continuity) equation. Water and landslide material are represented as fluids with different densities, and the landslide-water and

water-air interfaces are tracked using the Volume of Fluid (VOF) method. Once the tsunami wave is fully developed, the wave is passed as an initial condition to the 2D model for modeling wave propagation and coastal inundation. The generated wave is considered fully developed when the total wave energy (potential plus kinetic) reaches a maximum and before the wave leaves the computational domain, as discussed in López-Venegas et al. [2015]. The 2D model used here is NEOWAVE [Yamazaki et al., 2008], a depth-integrated and nonhydrostatic model built on the nonlinear shallow water equations. Propagation and inundation are calculated via a series of nested grids of increasing resolution, from 15 arcsecond ($\sim 450\text{m}$) resolution for a domain encompassing the entire northern GoM (Figure 1), to 3 arcsecond ($\sim 90\text{m}$) resolution (NOAA NCEI Coastal Relief Models), 1 arcsecond ($\sim 30\text{m}$) resolution, and 1/3 arcsecond ($\sim 10\text{m}$) resolution (NOAA NCEI Tsunami Inundation Digital Elevation Models [DEMs]) to model detailed inundation of the most populated/inundation-prone areas of each coastal community. The 3 arcsecond ($\sim 90\text{m}$) grids encompassing each coastal community studied here are shown by red rectangles in Figure 1.

2.2 Landslide Tsunami Sources

Seven large-scale landslide configurations were created assuming an unstable (gravity-driven) sediment deposit condition. Three of these landslide configurations are historical events identified by ten Brink et al. [2009]: the East Breaks, Mississippi Canyon, and West Florida submarine landslides (red hatched regions in Figure 1). The other four were obtained using a probabilistic methodology based on work by Marezki et al. [2007] and Grilli et al. [2009] and extended for the GoM by A. Pampell-Manis, *J. Geophys. Res. Oceans*, under review. Landslide configurations are determined based on distributions of previous GoM submarine landslide dimensions through a Monte Carlo Simulation (MCS) technique which incorporates a Cholesky decomposition method for correlated landslide size parameters. This method captures trends seen in the data while allowing for randomness in the generated landslide dimensions. Slope stability analyses are performed using landslide and sediment properties and regional seismic loading to determine landslide configurations which fail and produce a tsunami. The probability of each tsunamigenic failure is calculated based on the joint probability of slope failure and probability of the triggering earthquake. Those failures which produce the largest tsunami amplitude and have the highest probability of occurrence are deemed the most extreme probabilistic events, and the dimensions of these events are averaged to determine maximum credible probabilistic sources. The four maximum credible Probabilistic Submarine Landslides (PSLs) used here are termed PSL-A, PSL-B1, PSL-B2, and PSL-C (blue hatched regions in Figure 1). A complete discussion of the submarine landslide sources used here is given in Horrillo et al. [2015].

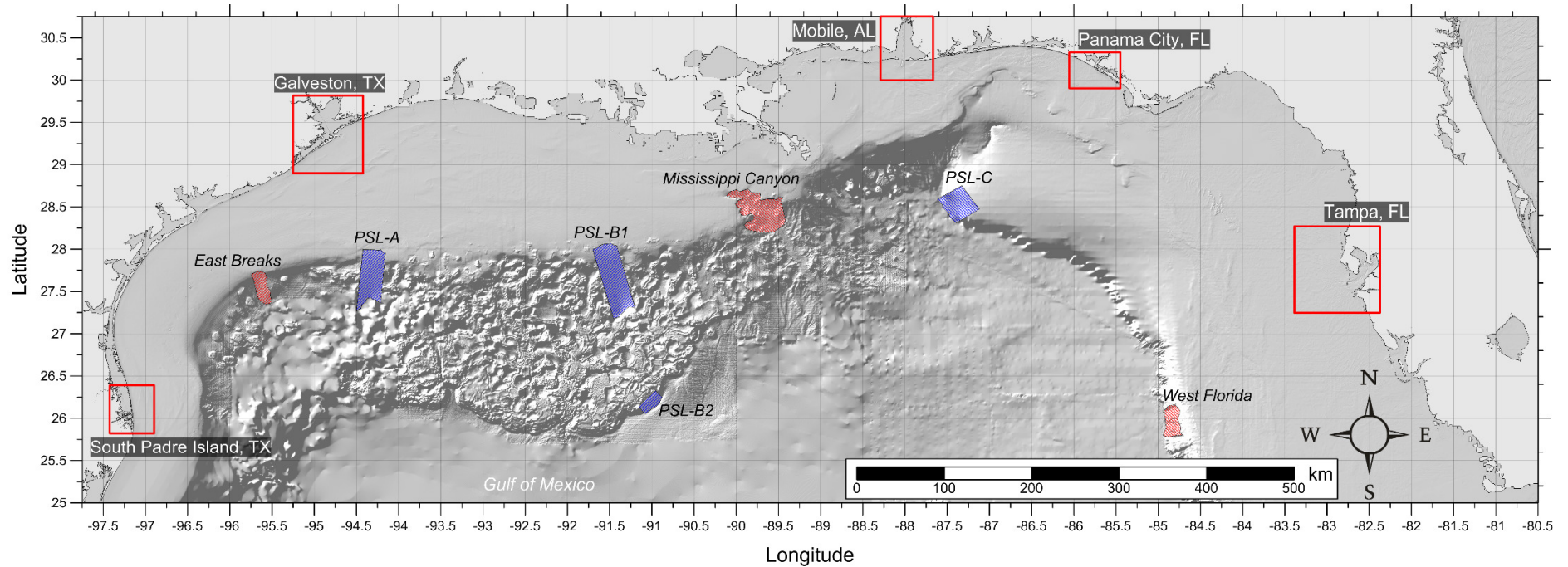


Figure 1: Northern Gulf of Mexico domain used in NEOWAVE to model wave propagation. Footprints of submarine landslides are shown as colored hatched regions: red regions correspond to identified historical failures; blue regions correspond to created probabilistic landslides. Red rectangles indicate 3 arcsecond ($\sim 90\text{m}$) domains of each coastal community where tsunami inundation is modeled. Contour drawn is the zero-meter contour for land elevation.

2.3 Inundation Maps and Comparison with Hurricane Storm Surge Inundation

Maximum inundation depth and extent are determined for each of the five coastal communities: South Padre Island, TX; Galveston, TX; Mobile, AL; Panama City, FL; and Tampa, FL. Elevations used are in reference to the Mean High Water (MHW) tidal datum, and inundation is determined by subtracting land elevation from water elevation. We model maximum-of-maximums (MOM) tsunami inundation depth/extent for each community, calculated as the maximum inundation depth from an ensemble of all seven tsunami sources considered here. That is, once inundation in a community has been modeled for each of the seven sources, we take the overall maximum inundation depth in each computational grid cell as the MOM tsunami inundation. This approach gives a worst-case scenario perspective of estimated tsunami inundation for each coastal community.

Due to the limitations on availability of high-resolution (1/3 arcsecond) DEMs, detailed inundation maps for all communities along the Gulf Coast are not yet possible. In an effort to develop a first-order estimate of potential tsunami inundation for those locations where detailed inundation maps have not yet been developed, we compare tsunami inundation to hurricane storm surge data. Along the Gulf Coast, hurricanes are a fairly regular threat, and hurricane preparedness approaches are well-developed. As a result, comparing tsunami inundation with hurricane storm surge provides a basis for tsunami preparedness efforts. The hurricane storm surge data used here is that available from the Sea, Lake, and Overland Surges from Hurricanes (SLOSH) model developed by the National Weather Service (NWS). The SLOSH model has been developed to provide estimates of storm surge heights caused by historical, predicted, or hypothetical hurricanes based on different values for atmospheric pressure, size, forward speed, and track data. It uses a polar, elliptical, or hyperbolic grid for computations, leading to higher resolutions near coastal areas of interest. The SLOSH results used here are the Maximum of Maximums (MOMs), which provide the worst-case storm surge for a given hurricane category and initial tide level based on a set of model runs with varying storm parameters.

The SLOSH MOM results at high tide are compared to the tsunami MOMs for each of the five mapped coastal communities. To perform the comparison, the SLOSH MOM output data was first converted to meters and adjusted to the MHW tidal datum. Then, SLOSH MOM inundation was determined by interpolating the SLOSH storm surge elevation to 1/3 arcsecond ($\sim 10\text{m}$) resolution and subtracting bathymetry/land elevation. Since severity of an anticipated hurricane is generally indicated by hurricane category, we aim to determine the hurricane category which produces MOM storm surge inundation ζ_h that is a best match to the tsunami MOM inundation ζ_t . That is, we determine the hurricane category which satisfies

$$\min_c (|\zeta_{h_c} - \zeta_t|), \quad c = \text{Cat}1, \dots, \text{Cat}5 \quad (1)$$

for each grid cell. The inundation level for that category is denoted $\zeta_{h_{min}}$. The actual difference between inundation levels $\Delta\zeta = \zeta_{h_{min}} - \zeta_t$ is also calculated to determine how close of a match the best-match category actually is. Thus, positive values of $\Delta\zeta$ indicate where hurricane storm surge inundation is higher than tsunami inundation, and negative values indicate where tsunami inundation is higher than hurricane storm surge inundation. Comparisons are only made where either the tsunami or hurricane MOM inundation is at least 0.3m ($\sim 1\text{ft}$); lower inundation is considered negligible here.

2.4 South Padre Island, TX

Figure 2 shows the MOM tsunami inundation for South Padre Island, TX. Note that inundation less than 0.3m (~ 1 ft) is not shown (same for all other figures of tsunami inundation). Clearly, the tsunami almost completely overtops the barrier island, as well as the northern part of the peninsula to the south. Highest inundation is seen at the beachfront, as could be expected, though significant inundation is seen across most of the island and peninsula past the dune system. Inundation also reaches across Laguna Madre to flood areas south of Port Isabel.

Figure 3 shows the hurricane category at high tide which best matches the tsunami inundation. Figure 4 shows $\Delta\zeta$ for the best-match hurricane category satisfying equation 1 and shown in Figure 3. Note that pale colors (pale orange and yellow) in Figure 4 indicate relatively good agreement between tsunami and storm surge inundation, i.e. $-0.5\text{m} \leq \Delta\zeta \leq 0.5\text{m}$.

Clearly, there is a trend of decreasing hurricane category from the beach toward inland regions, as could be expected. Most of the barrier island experiences tsunami inundation comparable to a Category 3 or higher hurricane, with greater than Category 5 inundation seen at the immediate beachfront, significantly greater in some places (up to 5m higher tsunami inundation than hurricane storm surge). Beyond the dune system, tsunami inundation is comparable to a Category 3-4, and at the lee part of the barrier island, tsunami inundation is on the order of a Category 3 hurricane. Across the channel/lagoon and into Port Isabel, tsunami inundation is on the order of a Category 1-2 hurricane.

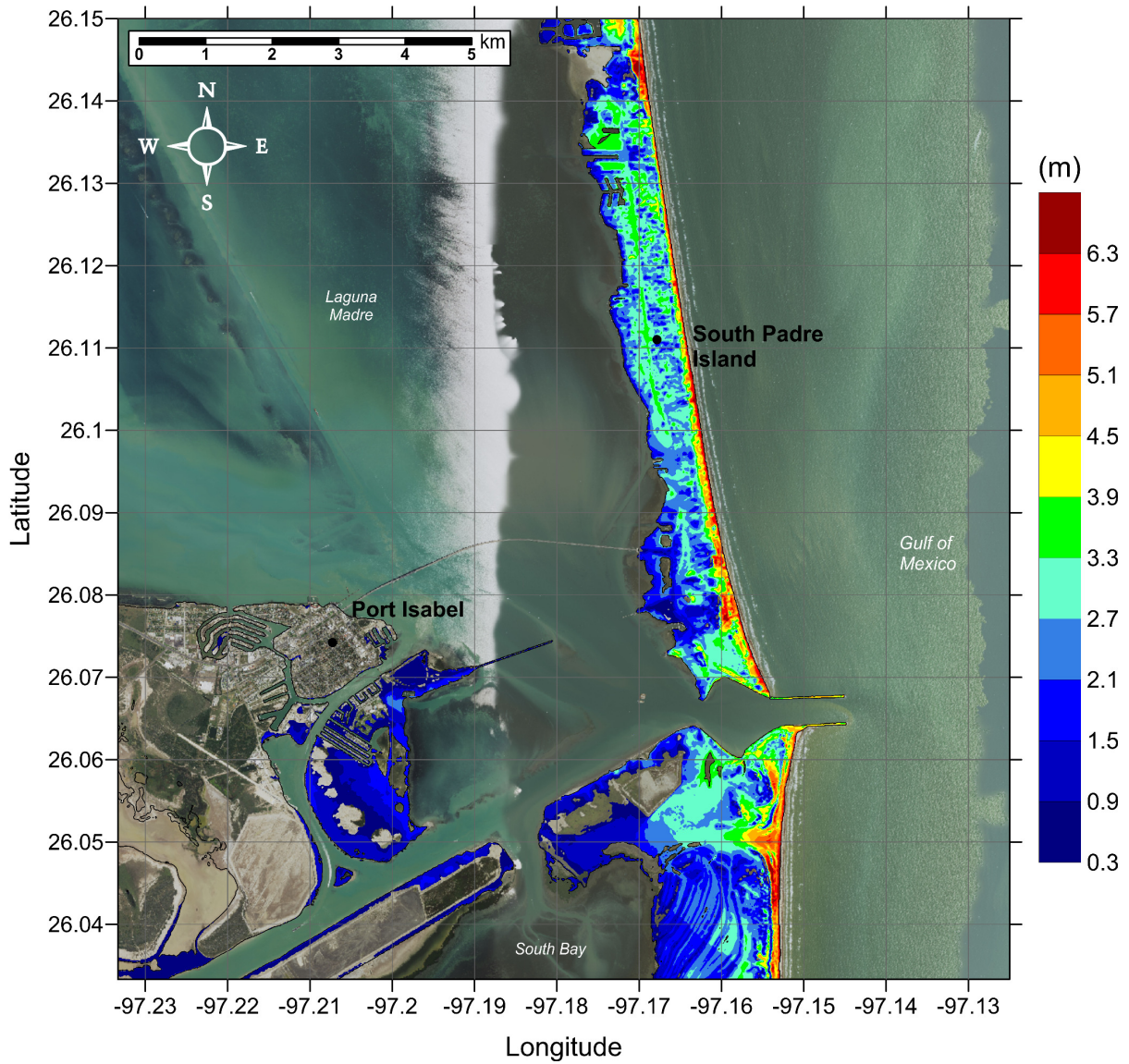


Figure 2: Maximum of maximums tsunami inundation depth (m) in South Padre Island, TX, calculated as the maximum inundation depth in each grid cell from an ensemble of all tsunami sources considered. Contour drawn is the zero-meter contour for land elevation.

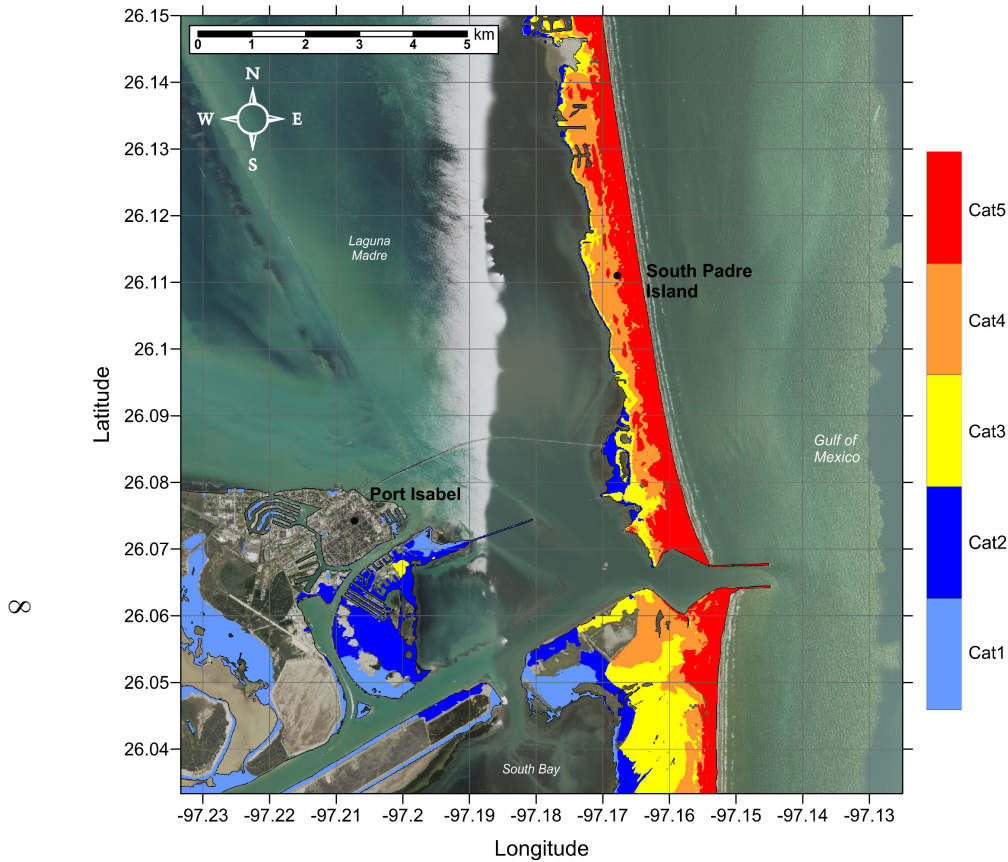


Figure 3: Hurricane category which produces inundation at high tide that best matches the MOM tsunami inundation shown in Figure 2 for South Padre Island, TX.

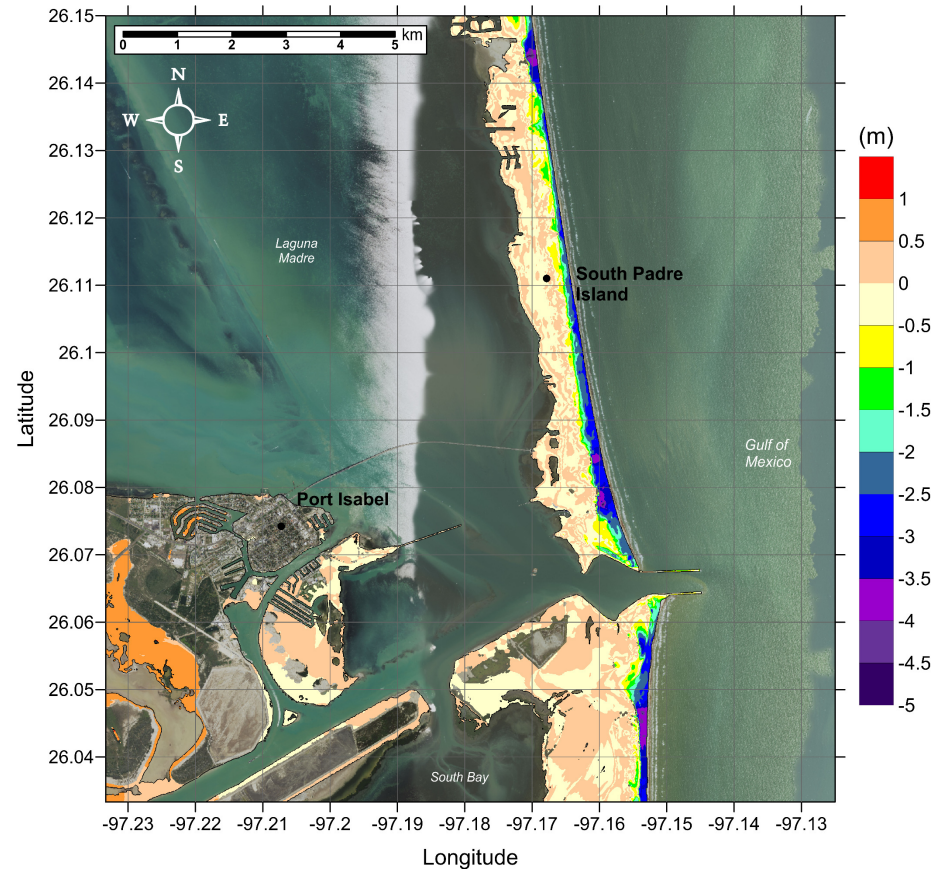


Figure 4: Actual difference $\Delta\zeta$ (m) between SLOSH MOM storm surge inundation and MOM tsunami inundation for the best-match hurricane category shown in Figure 3 for South Padre Island, TX. Note that negative values indicate where tsunami inundation is higher than hurricane inundation, and pale colors indicate relatively good agreement between tsunami and storm surge inundation, i.e. $|\Delta\zeta| \leq 0.5$ m.

2.5 Galveston, TX

Figure 5 shows the MOM tsunami inundation for Galveston, TX. The island is fairly well protected from tsunami inundation due to the seawall protecting the most populated part of the island, although the lower-lying areas at the east end of the island and to the west where the seawall is not present experience a higher hazard. Inundation also originates from the bay and channel at the lee part of the island, flooding portions of the northern shore.

Figure 6 shows the best-match hurricane category at high tide. Figure 7 shows $\Delta\zeta$ for the best-match hurricane category. Once again, pale colors (pale orange and yellow) in Figure 7 indicate relatively good agreement between tsunami and storm surge inundation, i.e. $|\Delta\zeta| \leq 0.5\text{m}$. Tsunami inundation is comparable to a Category 1 or 2 hurricane throughout the majority of the flooded regions of the island. Tsunami inundation on the order of a Category 3-4 hurricane is seen at the beachfront and in low-lying areas toward the east end of the island in front of the seawall. There is relatively good agreement between tsunami and hurricane inundation throughout the island ($|\Delta\zeta| \leq 0.5\text{m}$), with hurricane storm surge greater than tsunami inundation particularly toward the back part of the island where storm surge inundates from Galveston Bay and Offatts Bayou. Tsunami inundation is greater than that for hurricanes mostly toward the west end of the island that is not protected by the seawall.

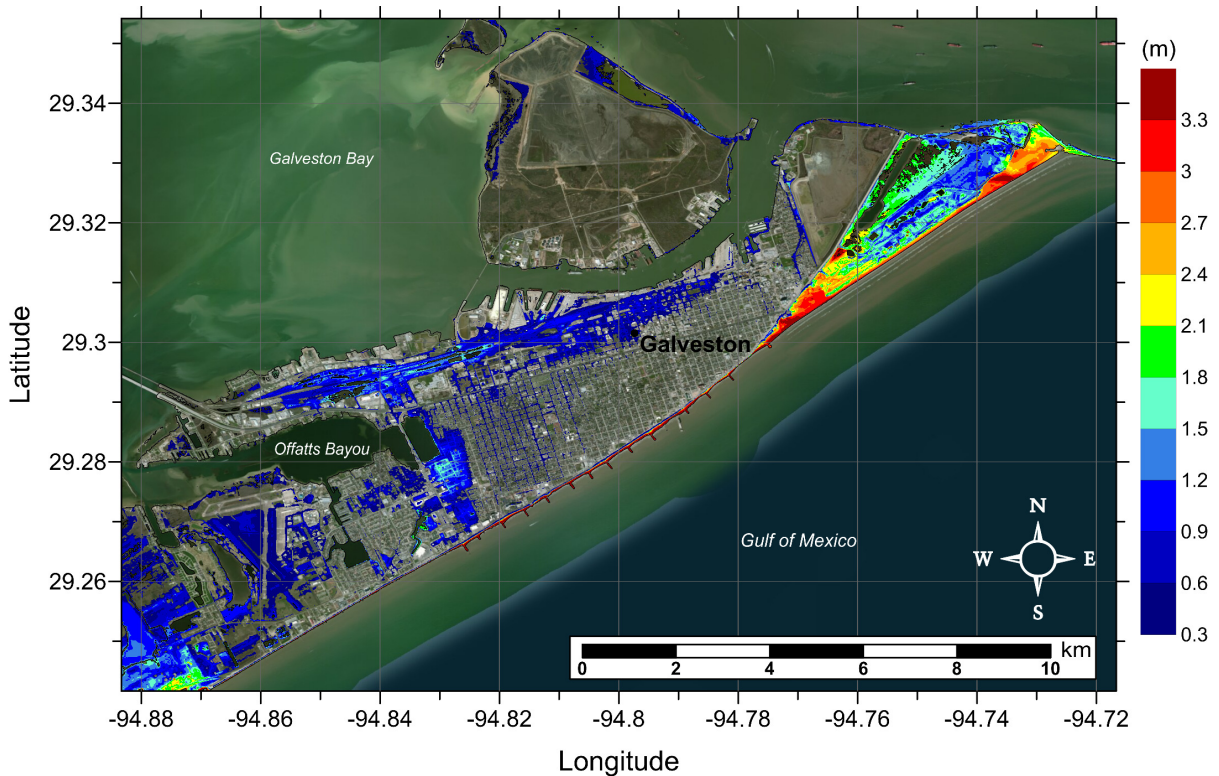


Figure 5: Maximum of maximums tsunami inundation depth (m) in Galveston, TX, calculated as the maximum inundation depth in each grid cell from an ensemble of all tsunami sources considered. Contour drawn is the zero-meter contour for land elevation.

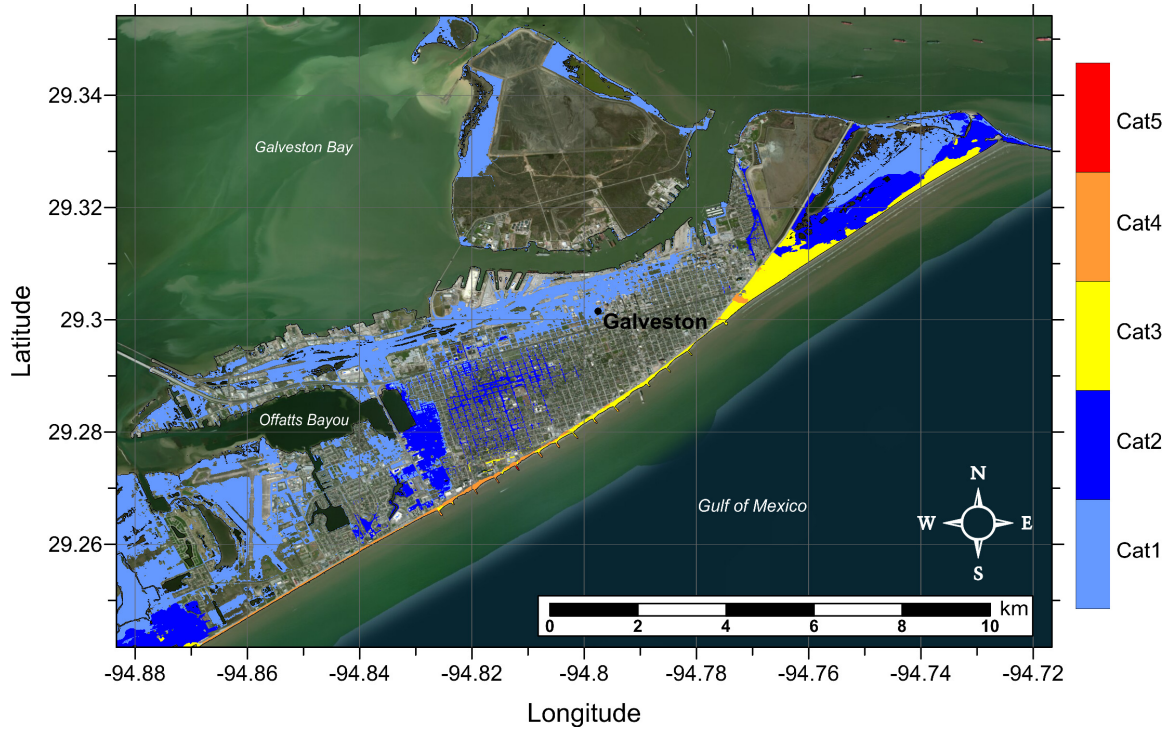


Figure 6: Hurricane category which produces inundation at high tide that best matches the MOM tsunami inundation shown in Figure 5 for Galveston, TX.

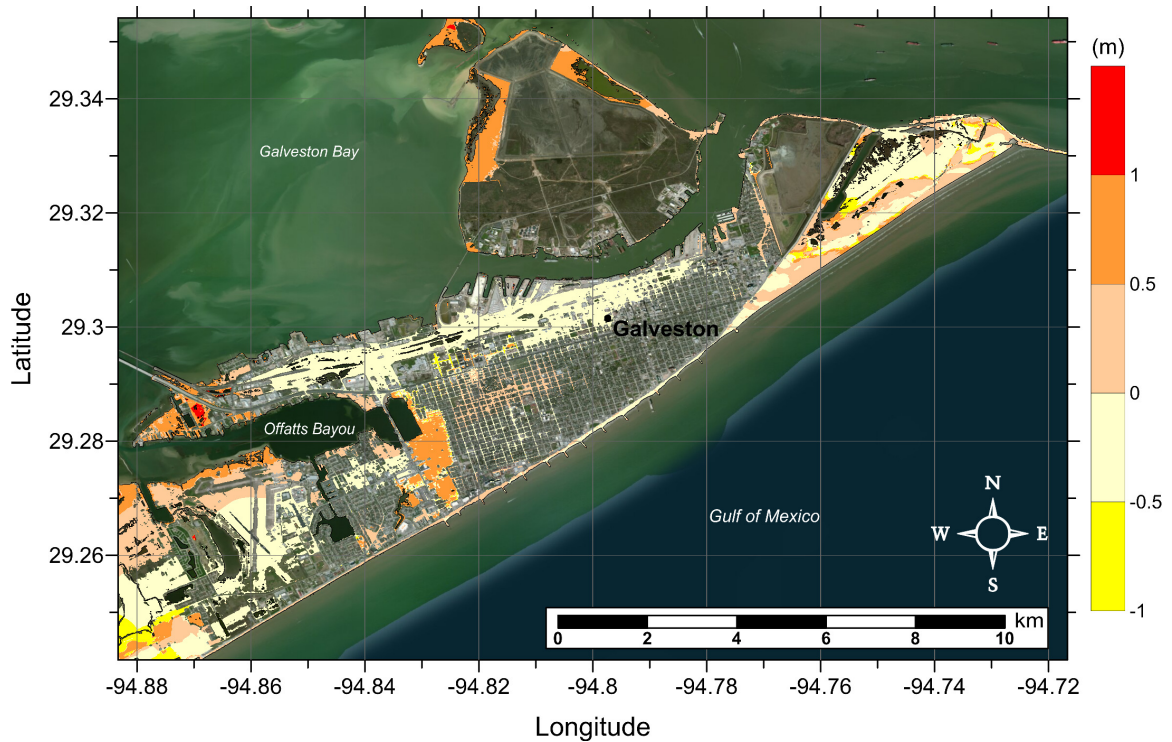


Figure 7: Actual difference $\Delta\zeta$ (m) between SLOSH MOM storm surge inundation and MOM tsunami inundation for the best-match hurricane category shown in Figure 6 for Galveston, TX. Note that negative values indicate where tsunami inundation is higher than hurricane inundation, and pale colors indicate relatively good agreement between tsunami and storm surge inundation, i.e. $|\Delta\zeta| \leq 0.5\text{m}$.

2.6 Mobile, AL

MOM tsunami inundation for the greater Mobile, AL region is given in Figures 8 and 11. Figure 8 shows inundation for Dauphin Island/Gulf Highlands, AL, at the mouth of Mobile Bay, and Figure 11 shows inundation in Mobile, AL proper. Dauphin Island/Gulf Highlands are almost completely overtopped by the tsunami, with the highest inundation seen at the beachfront, while Mobile itself is largely protected in its position at the northern end of Mobile Bay, with only minor tsunami inundation seen along the shores of the bay and inland waterways.

Figure 9 shows the best-match hurricane category with an initial high tide level for Dauphin Island/Gulf Highlands, AL. Figure 10 shows $\Delta\zeta$ for the best-match hurricane category. Crossing Dauphin Island and the peninsula of Gulf Highlands, there is a general decrease in hurricane category. Across the eastern part of Dauphin Island, tsunami inundation is comparable to a major hurricane: Category 4-5 hurricane at the beachfront and Category 3-4 at the eastern tip of the island. Category 1-2 levels are seen at the backside of this portion of the island. The western part of the island experiences tsunami inundation at Category 3-4 levels across the entire narrow strip of land. On the peninsula containing Gulf Highlands, tsunami inundation is greater than a Category 5 at the beachfront, significantly so (up to 5m higher) toward the east. Tsunami inundation is comparable to a Category 5 hurricane across much of the peninsula, decreasing to a Category 2-3 at the western portion of the lee part of the peninsula, though Category 4 levels are still seen at the eastern part of the backside of the peninsula.

Figures 12-13 show the best-match high tide hurricane category and $\Delta\zeta$ for the best-match hurricane category, respectively, for Mobile, AL. While Mobile is threatened by hurricane storm surge due to Mobile Bay and the numerous rivers and inland waterways, its position at the north of Mobile Bay provides protection from significant tsunami inundation; tsunami inundation is mostly less than that for a Category 1 hurricane.

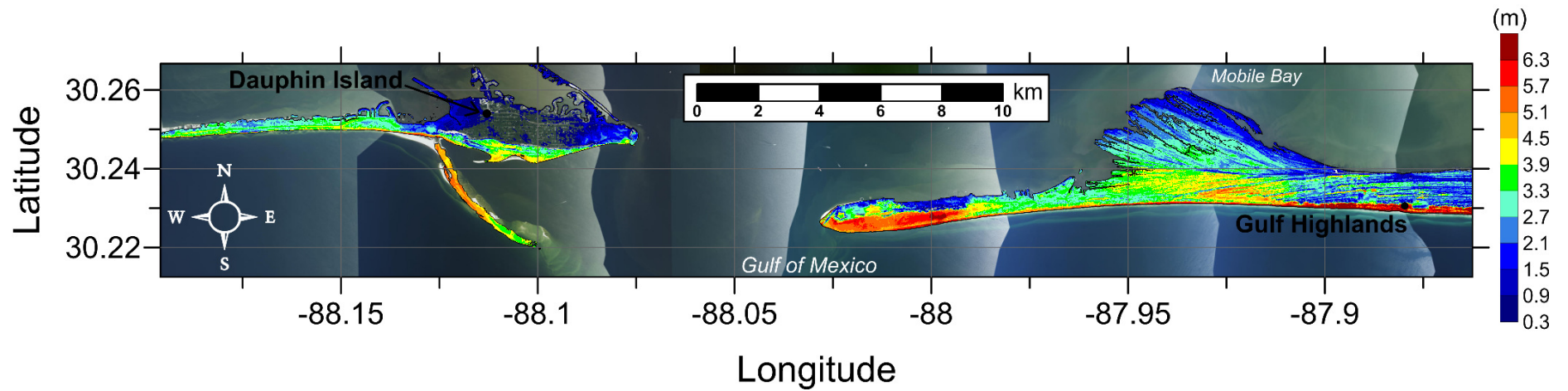


Figure 8: Maximum of maximums tsunami inundation depth (m) in Dauphin Island/Gulf Highlands, AL, calculated as the maximum inundation depth in each grid cell from an ensemble of all tsunami sources considered. Contour drawn is the zero-meter contour for land elevation.

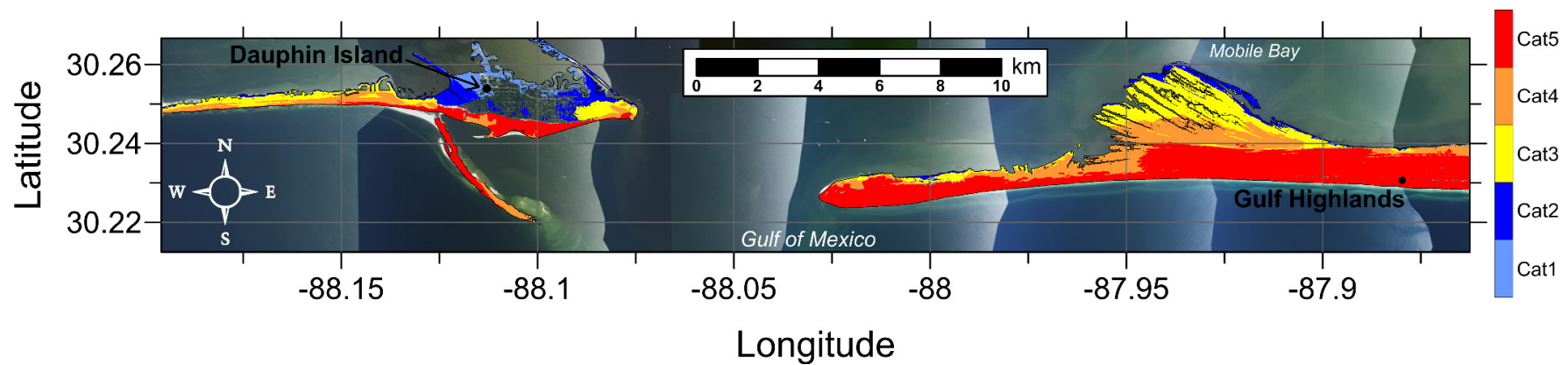


Figure 9: Hurricane category which produces inundation at high tide that best matches the MOM tsunami inundation shown in Figure 8 for Dauphin Island/Gulf Highlands, AL.

13

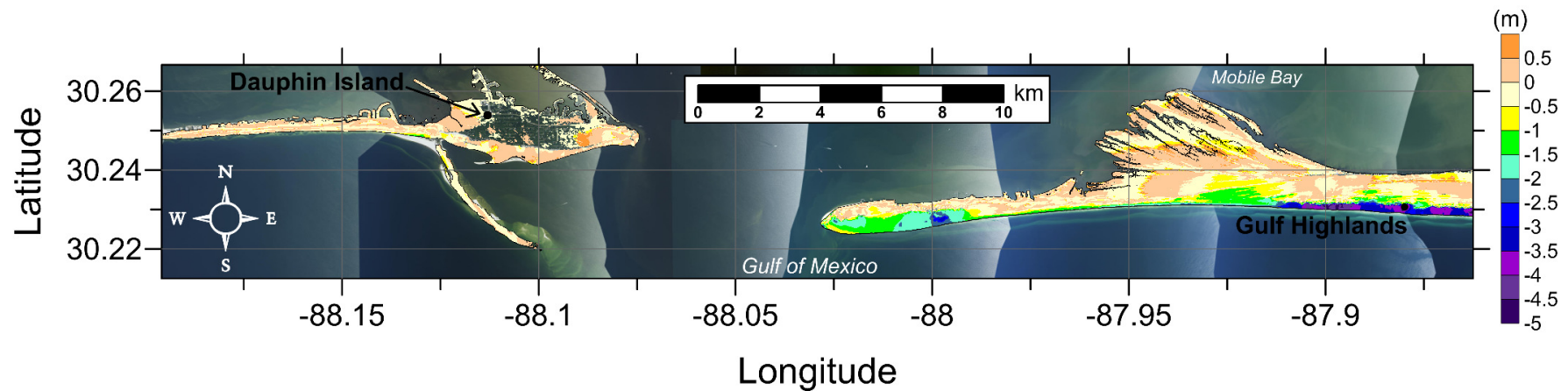


Figure 10: Actual difference $\Delta\zeta$ (m) between SLOSH MOM storm surge inundation and MOM tsunami inundation for the best-match hurricane category shown in Figure 9 for Dauphin Island/Gulf Highlands, AL. Note that negative values indicate where tsunami inundation is higher than hurricane inundation, and pale colors indicate relatively good agreement between tsunami and storm surge inundation, i.e. $|\Delta\zeta| \leq 0.5\text{m}$.

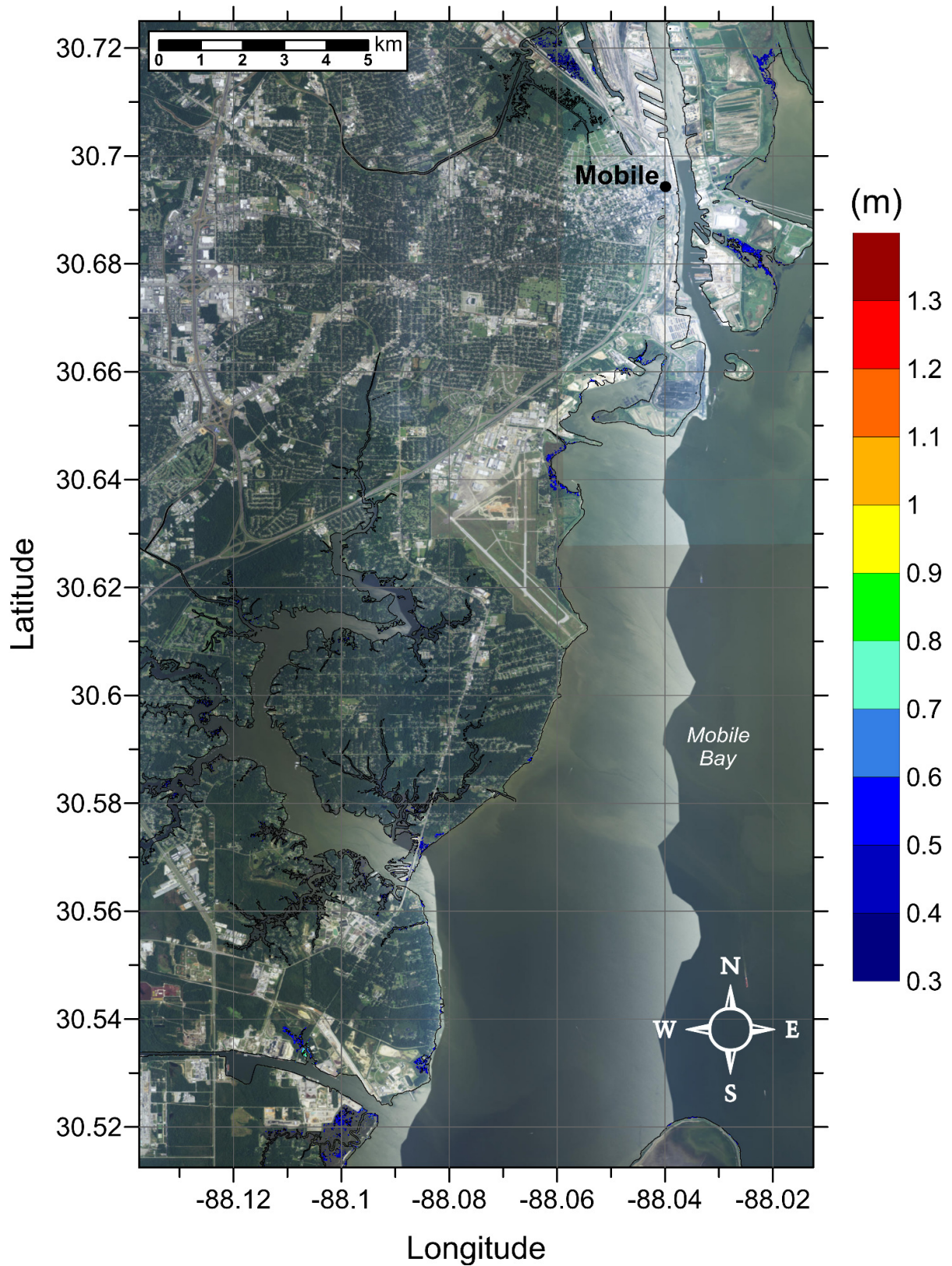


Figure 11: Maximum of maximums tsunami inundation depth (m) in Mobile, AL, calculated as the maximum inundation depth in each grid cell from an ensemble of all tsunami sources considered. Contour drawn is the zero-meter contour for land elevation.

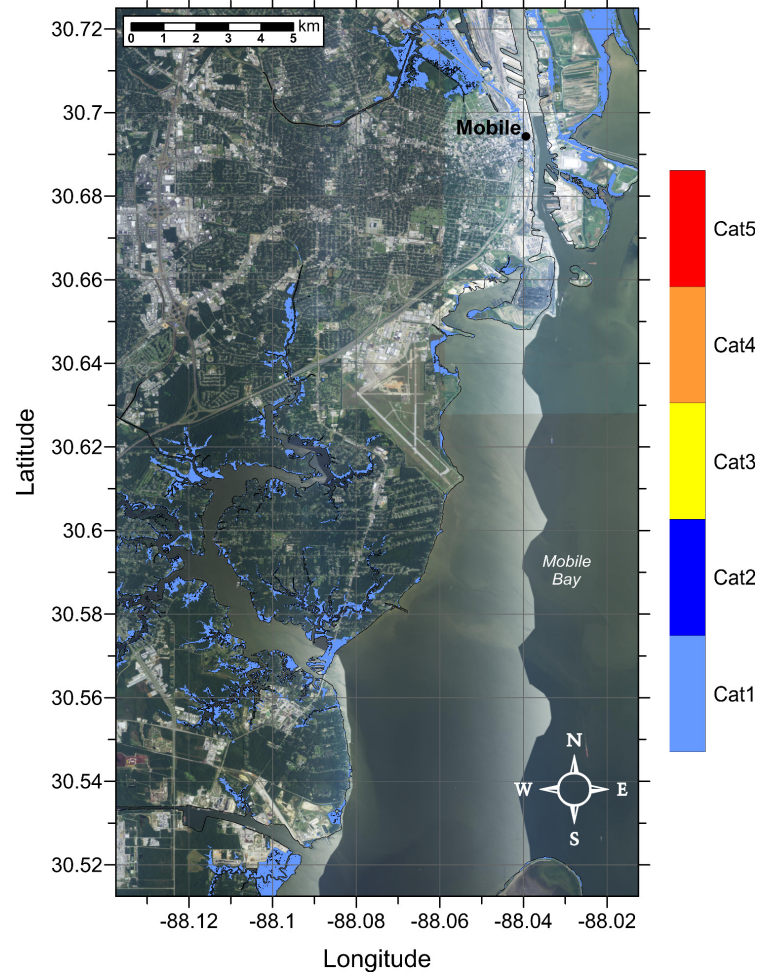


Figure 12: Hurricane category which produces inundation at high tide that best matches the MOM tsunami inundation shown in Figure 11 for Mobile, AL.

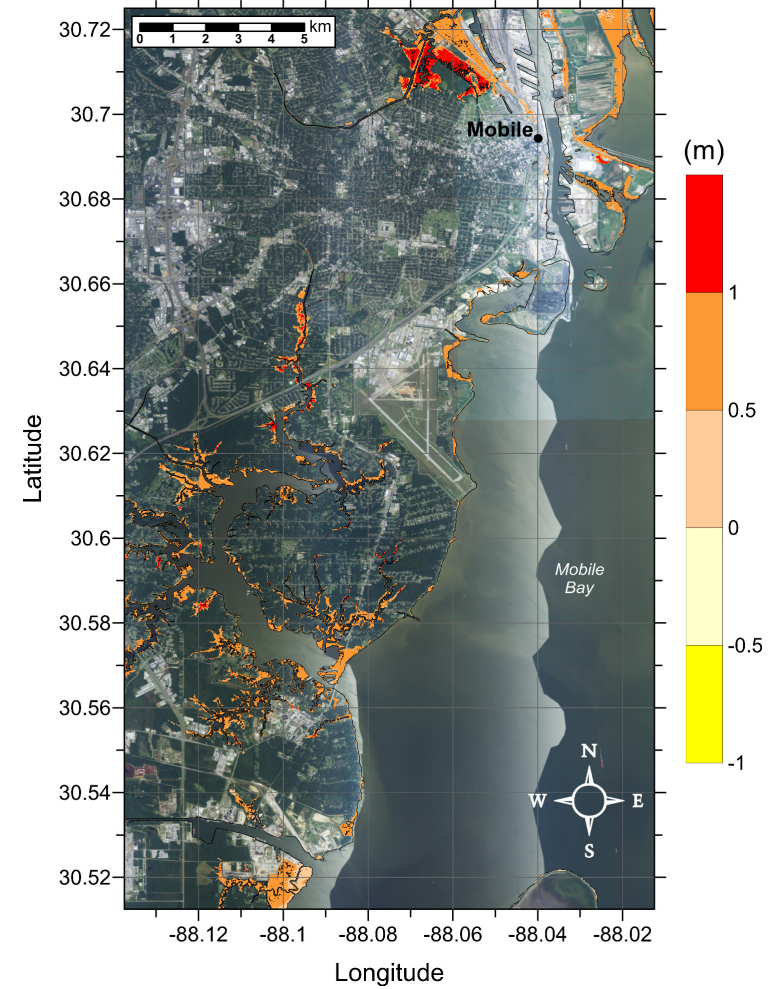


Figure 13: Actual difference $\Delta\zeta$ (m) between SLOSH MOM storm surge inundation and MOM tsunami inundation for the best-match hurricane category shown in Figure 12 for Mobile, AL. Note that negative values indicate where tsunami inundation is higher than hurricane inundation, and pale colors indicate relatively good agreement between tsunami and storm surge inundation, i.e. $|\Delta\zeta| \leq 0.5\text{m}$.

2.7 Panama City, FL

Figure 14 shows MOM tsunami inundation for the greater Panama City, FL region. This region experiences widespread tsunami inundation with significant (greater than 6.3m, ~ 21 ft) inundation depth at the beachfront and overtopping the dune system. Inundation depths of up to 1.5 m are seen reaching 5 km inland of the beachfront. This is most likely due to water traveling from low-lying areas northwest of Panama City Beach. Inundation also originates from inland waterways such as the Grand Lagoon.

Figure 15 shows the best-match hurricane category at high tide and Figure 16 shows $\Delta\zeta$ for the best-match hurricane category. Overall, tsunami inundation is comparable to a major hurricane throughout most of this domain. Throughout most of the beachfront area and reaching well inland, tsunami inundation is significantly greater than a Category 5 hurricane (up to 8.5m higher than the storm surge inundation in some beach areas). Comparable hurricane category steadily decreases from Category 5 to Category 2 moving north starting approximately 4km inland. Around the Grand Lagoon, tsunami inundation is on the order of a Category 3-5 hurricane, and across St. Andrew Bay along the mainland coast, tsunami inundation is comparable to Category 2-3 levels.

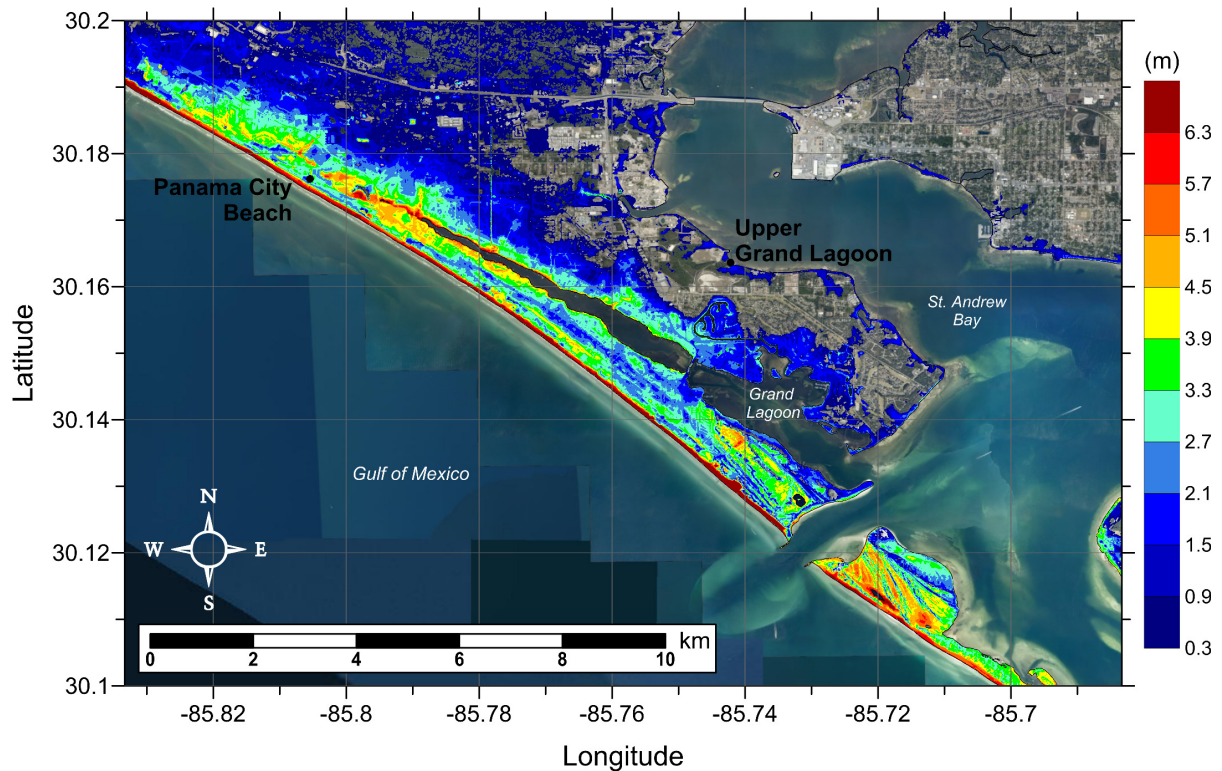


Figure 14: Maximum of maximums tsunami inundation depth (m) in the Panama City Beach, FL region, calculated as the maximum inundation depth in each grid cell from an ensemble of all tsunami sources considered. Contour drawn is the zero-meter contour for land elevation.

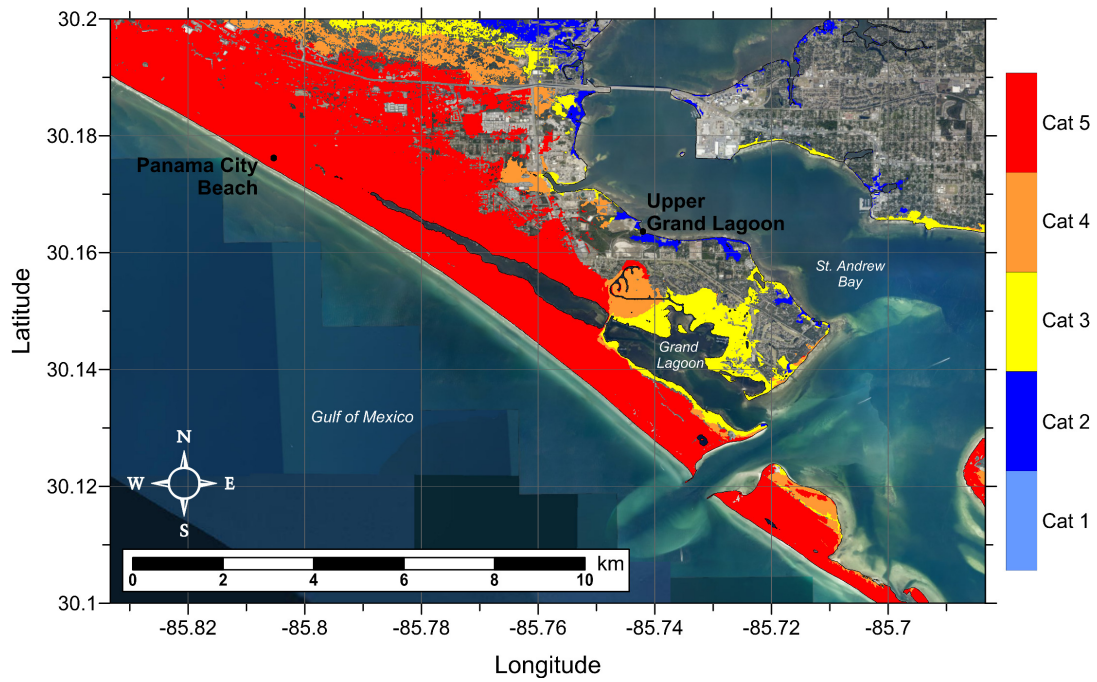


Figure 15: Hurricane category which produces inundation at high tide that best matches the MOM tsunami inundation shown in Figure 14 for the Panama City Beach, FL region.

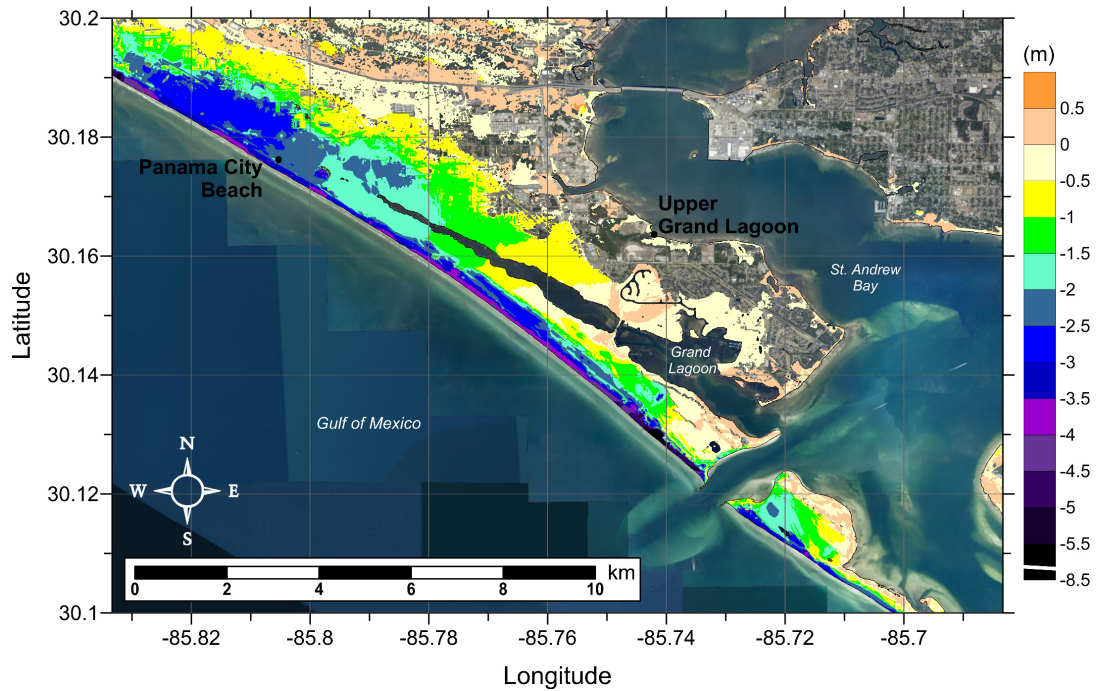


Figure 16: Actual difference $\Delta\zeta$ (m) between SLOSH MOM storm surge inundation and MOM tsunami inundation for the best-match hurricane category shown in Figure 15 for the Panama City Beach, FL region. Note that negative values indicate where tsunami inundation is higher than hurricane inundation, and pale colors indicate relatively good agreement between tsunami and storm surge inundation, i.e. $|\Delta\zeta| \leq 0.5\text{m}$.

2.8 Tampa, FL

MOM tsunami inundation for the greater Tampa - St. Petersburg - Clearwater area is given in Figures 17-18. The numerous canals and waterways in Tampa provide many possible trajectories for tsunami waves to inundate the small residential islands in this community, but also many obstacles to dissipate tsunami energy. As a result, the most inundation is seen in the northern greater Tampa region (Figure 18) where the mainland is in close proximity to the barrier islands and the highest tsunami energy. The southern greater Tampa region (Figure 17) experiences inundation mostly along the immediate beachfront and in some small islands forming the inland canals behind the main barrier island.

Figures 19 and 20 show the high tide best-match hurricane category and $\Delta\zeta$, respectively, for the southern part of the greater Tampa - St. Petersburg - Clearwater area. Figures 21 and 22 show the same for the northern part of the greater Tampa - St. Petersburg - Clearwater area. Tsunami inundation throughout both of these regions is comparable to a Category 1-3 hurricane: in general, Category 3 at the beachfront decreasing to Category 1 at the lee part of the barrier islands and inland across the various bays and inlets. The area around Indian Shores, in the northern greater Tampa - St. Petersburg - Clearwater area (Figure 21) also experiences tsunami inundation on the order of a Category 3 hurricane reaching approximately 1km inland on the mainland. This is most likely due to a focusing of tsunami energy at this location and the close proximity of the mainland to the barrier island.

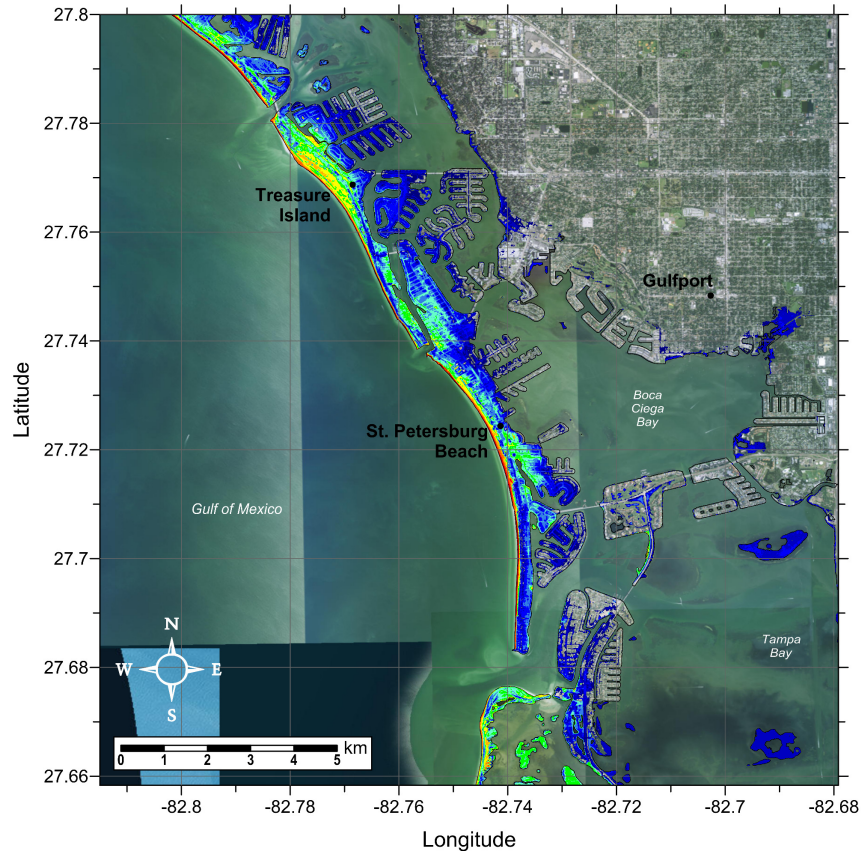


Figure 17: Maximum of maximums tsunami inundation depth (m) in the southern greater Tampa - St. Petersburg - Clearwater area, calculated as the maximum inundation depth in each grid cell from an ensemble of all tsunami sources considered. Contour drawn is the zero-meter contour for land elevation.

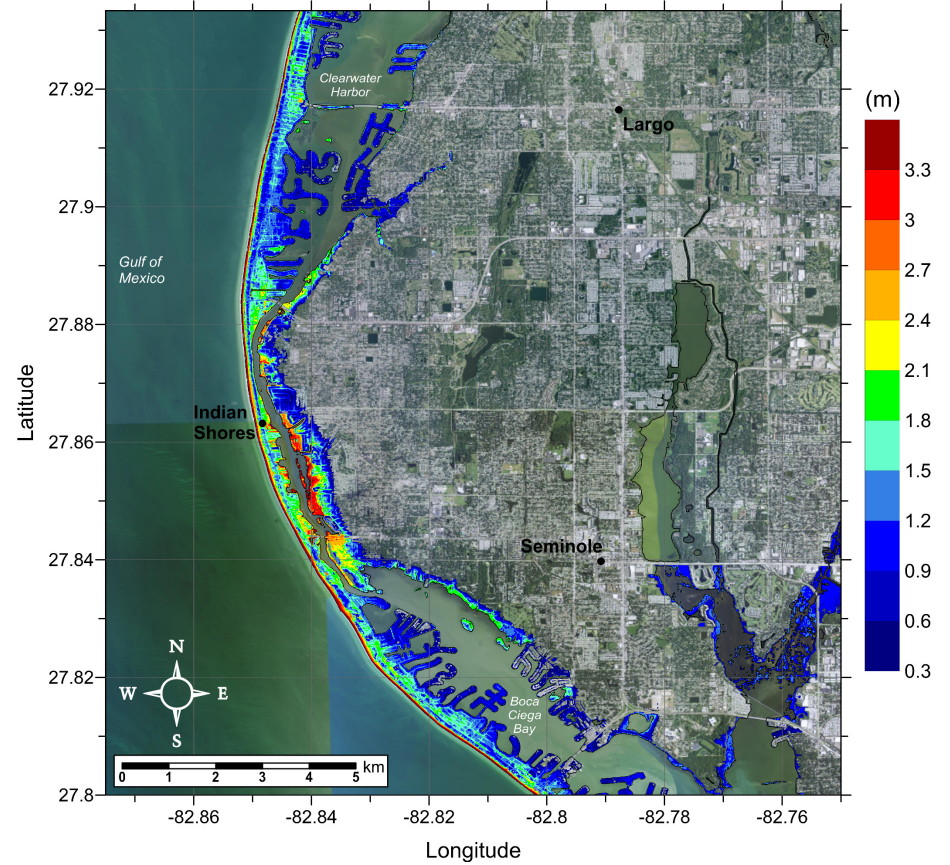


Figure 18: Maximum of maximums tsunami inundation depth (m) in the northern greater Tampa - St. Petersburg - Clearwater area, calculated as the maximum inundation depth in each grid cell from an ensemble of all tsunami sources considered. Contour drawn is the zero-meter contour for land elevation.

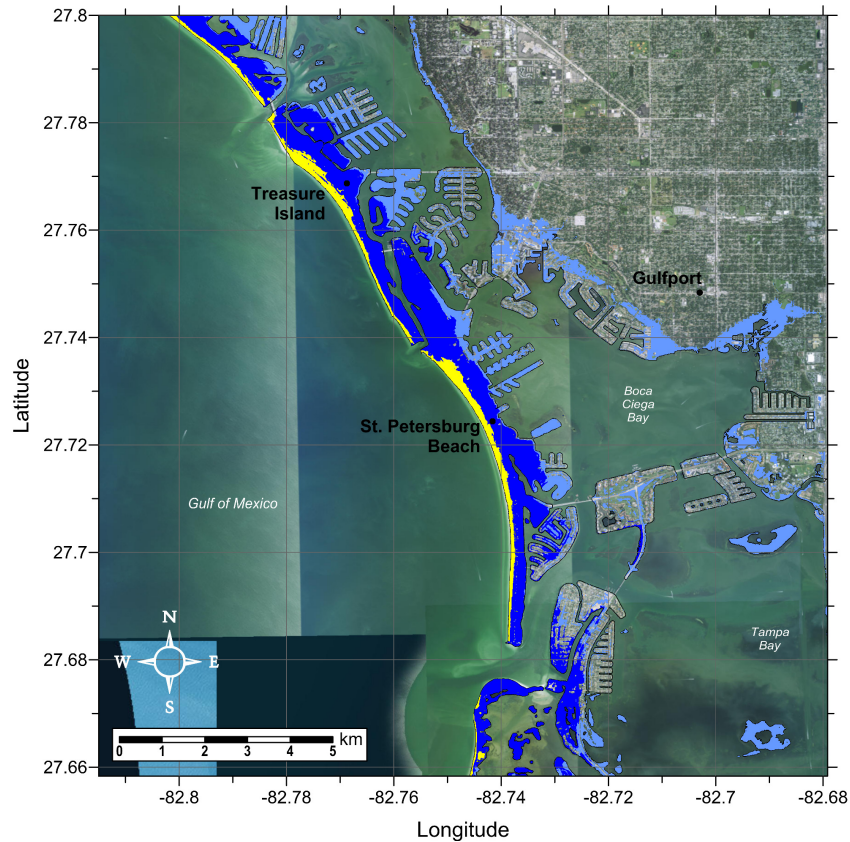


Figure 19: Hurricane category which produces inundation at high tide that best matches the MOM tsunami inundation shown in Figure 17 for the southern greater Tampa - St. Petersburg - Clearwater area.

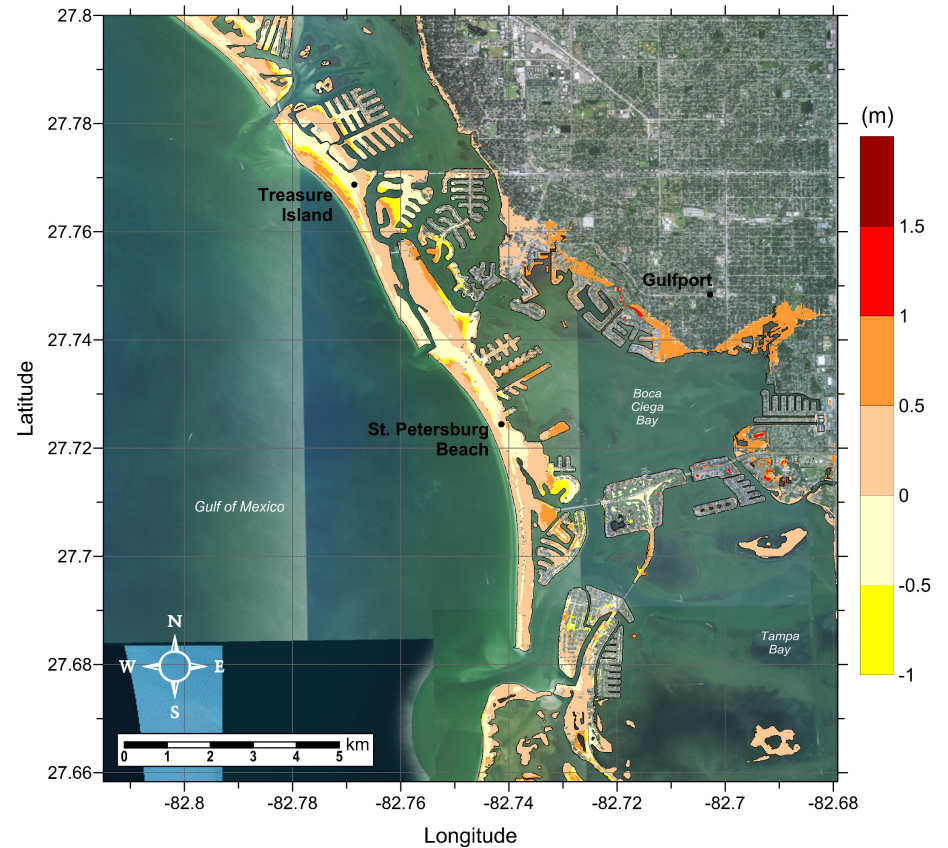


Figure 20: Actual difference $\Delta\zeta$ (m) between SLOSH MOM storm surge inundation and maximum-of-maximums tsunami inundation for the best-match hurricane category shown in Figure 19 for the southern greater Tampa - St. Petersburg - Clearwater area. Note that negative values indicate where tsunami inundation is higher than hurricane inundation, and pale colors indicate relatively good agreement between tsunami and storm surge inundation, i.e. $|\Delta\zeta| \leq 0.5\text{m}$.

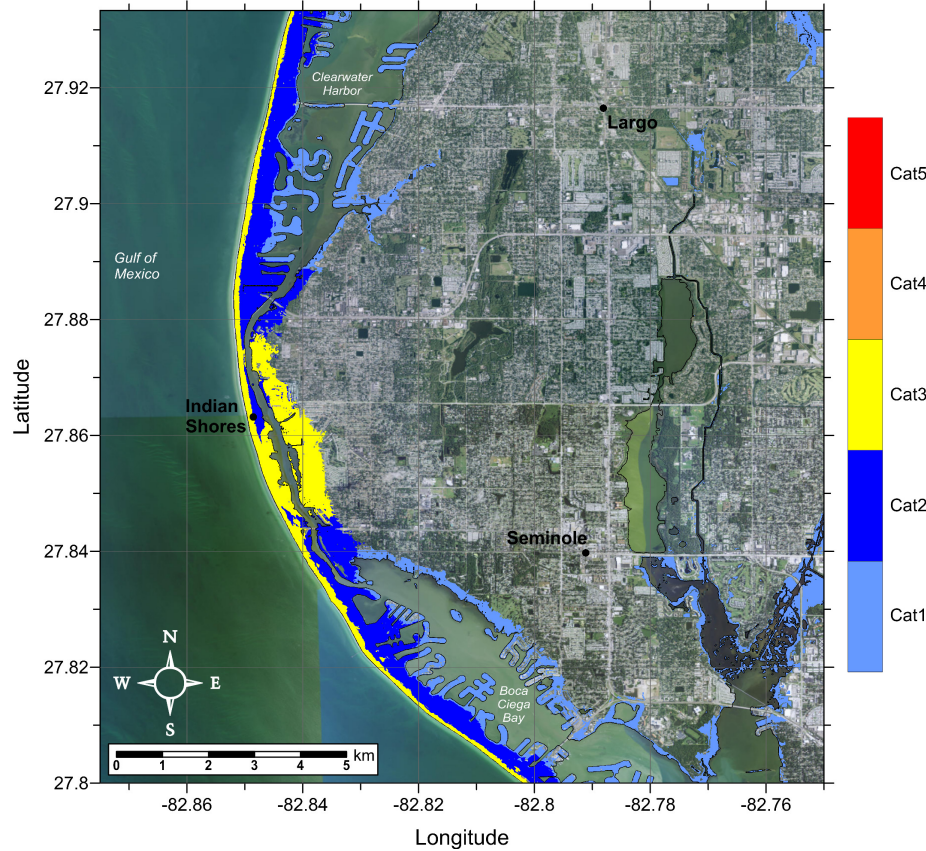


Figure 21: Hurricane category which produces inundation at high tide that best matches the MOM tsunami inundation shown in Figure 18 for the northern greater Tampa - St. Petersburg - Clearwater area.

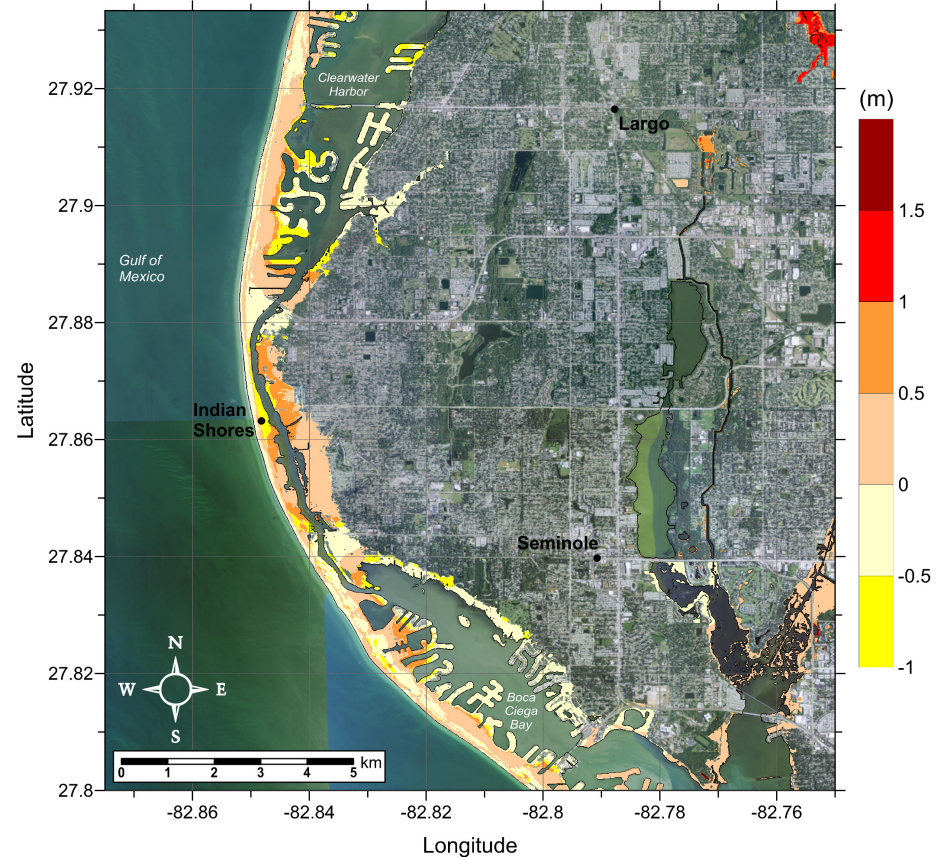


Figure 22: Actual difference $\Delta\zeta$ (m) between SLOSH MOM storm surge inundation and maximum-of-maximums tsunami inundation for the best-match hurricane category shown in Figure 21 for the northern greater Tampa - St. Petersburg - Clearwater area. Note that negative values indicate where tsunami inundation is higher than hurricane inundation, and pale colors indicate relatively good agreement between tsunami and storm surge inundation, i.e. $|\Delta\zeta| \leq 0.5$ m.

3 Conclusions

Tsunami inundation in five communities was modeled considering seven submarine landslide sources spread across the northern GoM. Level and extent of MOM tsunami inundation in each community varies depending on the regional variations in bathymetry/elevation. South Padre Island, TX, Dauphin Island/Gulf Highlands, AL, and Panama City, FL received the most inundation, in both depth and extent, overall. We see the most widespread inundation in Panama City. Galveston, TX is fairly well protected from inundation due to the seawall protecting the most populated part of the island. Most inundation in the greater Tampa - St. Petersburg - Clearwater area is seen to the north, while in the south inundation occurs mostly along the immediate beachfront and in some small islands behind the main barrier island. Mobile, AL itself is largely protected from tsunami inundation by its position at the northern end of Mobile Bay.

Comparisons of MOM tsunami inundation to the SLOSH MOM high tide inundation indicate that referencing to hurricane storm surge is location-specific, though some general regional trends can be identified. Immediate beachfront areas are inundated at levels comparable to major hurricanes, Category 3 or higher, with some places (particularly barrier islands and near where the continental shelf is relatively narrow, e.g. South Padre Island, TX, Dauphin Island/Gulf Highlands, AL, and Panama City, FL) experiencing tsunami inundation that is well above Category 5 levels (up to 5m higher or more). Where the continental shelf is wide or where the community is located more inland (e.g. Galveston, TX, Mobile, AL, and the greater Tampa, FL area), tsunami inundation depths seem to be comparable in general to a Category 3 hurricane at the immediate beachfront, with small stretches of Category 4 levels, and down to a Category 1 in more inland areas. However, it is worth noting that for Galveston, if the seawall were not present, it is possible that the hurricane comparison would be similar to the other barrier islands of South Padre Island and Dauphin Island/Gulf Highlands.

Overall, this study suggests that comparing tsunami and hurricane storm surge inundation seems to be a reasonable effort in order to provide low-resolution hazard zone information for Gulf Coast communities which do not currently warrant high-resolution tsunami inundation maps. While we acknowledge that storm surge characteristics (time scale, triggering mechanism, inundation process, etc.) are notably different than those of inundation caused by tsunamis, the correlations between tsunami and storm surge inundation are in general relatively good for the communities studied here and provide a generalized method for identifying hazard zones that is more appropriate for the Gulf Coast than methods such as the 10m (33ft) elevation contour line. Since even general, low-resolution inundation information is useful for hazard management planning, we believe that these results can be extended to provide a preliminary, first-order estimate of potential tsunami hazard level for other Gulf Coast communities where detailed tsunami inundation maps have not yet been developed or are not yet possible. We stress, however, that such results should be used only in a broad, regional sense given the differences seen among communities based on local details of bathymetry, land elevation, and geographical location within the GoM basin.

Acknowledgments

Funding for this work was provided by the National Tsunami Hazard Mitigation Program (NTHMP) under awards NA12NWS4670014, Construction of Five Additional Tsunami Inun-

dation Maps for the GOM; NA13NWS4670018, A Probabilistic Methodology for Hazard Assessment Generated by Submarine Landslide in the GOM; and NA14NWS4670049, Implementing NTHMP-MMS Strategic Plan in Tsunami Hazard Mitigation Products for the Gulf of Mexico. The authors also wish to thank Chayne Sparagowski and Amy Godsey for their direction on hurricane storm surge comparisons, and Craig Harter for his assistance with initial comparisons to storm surge data.

References

- P. K. Dunbar and C. S. Weaver. U.S. states and territories national tsunami hazard assessment: Historic record and sources for waves. Technical report, National Tsunami Hazard Mitigation Program, NOAA, U. S. Geol. Surv., 2008.
- E. L. Geist, J. D. Chaytor, T. Parsons, and U. ten Brink. Estimation of submarine mass failure probability from a sequence of deposits with age dates. *Geosphere*, 9(2):287–298, 2013.
- S. T. Grilli, O-D. S. Taylor, C. D. P. Baxter, and S. Marezki. A probabilistic approach for determining submarine landslide tsunami hazard along the upper east coast of the United States. *Mar. Geol.*, 264:74–97, 2009.
- J. Horrillo. *Numerical Method for Tsunami calculations using Full Navier-Stokes equations and the Volume of Fluid method*. PhD thesis, University of Alaska Fairbanks, 2006.
- J. Horrillo, A. Wood, G.-B. Kim, and A. Parambath. A simplified 3-D Navier-Stokes numerical model for landslide-tsunami: Application to the Gulf of Mexico. *J. Geophys. Res. Oceans*, 118:6934–6950, 2013.
- J. Horrillo, A. Pampell-Manis, C. Sparagowski, L. Parambath, and Y. Shigihara. Construction of five tsunami inundation maps for the Gulf of Mexico. Technical report, National Tsunami Hazard Mitigation Program, 2015.
- W. Knight. Model predictions of Gulf and Southern Atlantic Coast tsunami impacts from a distribution of sources. *Science of Tsunami Hazards*, 24:304–312, 2006.
- Alberto M. López-Venegas, Juan Horrillo, Alyssa Pampell-Manis, Victor Huérfano, and Aurelio Mercado. Advanced tsunami numerical simulations and energy considerations by use of 3D - 2D coupled models: The October 11, 1918, Mona Passage tsunami. *Pure Appl. Geophys.*, 172(6):1679–1698, 2015.
- S. Marezki, S. Grilli, and C. D. P. Baxter. Probabilistic SMF tsunami hazard assessment for the upper east coast of the United States. In V. Lykousis, D. Sakellariou, and J. Locat, editors, *Submarine Mass Movements and Their Consequences*, pages 377–385. Springer, 2007.
- U. S. ten Brink, D. Twichell, P. Lynett, E. Geist, J. Chaytor, H. Lee, B. Buczkowski, and C. Flores. Regional assessment of tsunami potential in the Gulf of Mexico. Technical report, National Tsunami Hazard Mitigation Program, U. S. Geol. Surv. Admin. Rep., 2009.
- Y. Yamazaki, Z. Kowalik, and K. F. Cheung. Depth-integrated, non-hydrostatic model for wave breaking and run-up. *Int. J. Numer. Meth. Fluids*, 61:473–497, 2008.